# Fast Adaptive Regularization for Perfusion Parameter Computation

## Tuning the Tikhonov Regularization Parameter to the SNR by Regression

Michael Manhart[1,2], Andreas Maier[2,3], Joachim Hornegger[2,3], Arnd Doerfler[1]

[1]Department of Neuroradiology, Universitätsklinikum Erlangen
[2]Pattern Recognition Lab, Friedrich-Alexander-Universität Erlangen-Nürnberg
[3]Erlangen Graduate School in Advanced Optical Technologies (SAOT), Erlangen
michael.manhart@cs.fau.de

**Abstract.** Computation of perfusion parameters by deconvolution from contrast-enhanced time-resolved CT or MR perfusion data sets is an ill-conditioned problem. Thus, adequate regularization and determination of corresponding regularization parameters is required. We present a novel method for Tikhonov regularization for perfusion imaging to locally adapt parameters to the SNR level by using a regression function. In an numerical evaluation our simple approach provided similar or even superior results compared to methods applying computationally more demanding L-curve analysis.

## 1 Introduction

Perfusion imaging techniques are widely used for diagnosis of cerebrovascular disease such as acute stroke as well as in the diagnostic work-up and therapy monitoring of brain tumors. Perfusion imaging is usually performed by contrast-enhanced time-resolved CT or MR imaging [1]. Recently, first results on interventional perfusion imaging using flat detector CT have been presented [2,3]. Perfusion parameters, such as the cerebral blood flow (CBF), can be computed by deconvolution techniques. In practice, the deconvolution process is performed by inversion of an ill-conditioned linear equation system (LES). To obtain a meaningful solution from the ill-conditioned inversion, Tikhonov regularization is commonly applied [1]. A crucial problem in regularization is how to choose the right parameter to control the trade-off between the regularization penalty and the data fit. In perfusion imaging, a fixed parameter independent of the contrast signal strength is usually used [1]. Salehi Ravesh et al. [4] showed that using an adaptive regularization parameter, which is tuned to the local signal-to-noise ratio (SNR), can improve MR lung perfusion measurements. The parameters are tuned locally by a modified version of the L-curve criterion (LCC) [5]. The LCC is a popular tool to find an appropriate parameter for Tikhonov regularization.

However, using L-curve analysis for determining adaptive regularization parameters causes a considerable amount of computational overhead. In this work,

we present a novel technique to adapt the regularization parameter locally to the SNR in a computationally efficient way by regression and show its potential benefits in a numerical brain perfusion phantom study.

## 2 Materials & Methods

### 2.1 Perfusion Parameter Computation using Tikhonov Regularization

The indicator-dilution theory describes how CBF and other related perfusion parameters can be recovered from the acquired time series of contrast agent enhanced volumes. For a comprehensive introduction, please refer to the review paper by Fieselmann et al. [1]. In this work, we restrict the description to the deconvolution problem, which needs to be solved by algebraic methods. We assume that the contrast agent attenuation is sampled at $t_i$, $i = 1 \dots N$ time points with a sampling distance $\Delta t$. Let matrix $\mathbf{A} \in \mathbb{R}^{N \times N}_{[0,\infty)}$ denote a convolution with the arterial input function (AIF), vector $\mathbf{c} \in \mathbb{R}^{N}_{[0,\infty)}$ a time-contrast-concentration curve (TCC) inside a tissue voxel, and vector $\mathbf{r} \in \mathbb{R}^{N}_{[0,\infty)}$ the corresponding residual function from which the essential perfusion parameters can be computed

$$\mathbf{A} = \Delta t \begin{pmatrix} a(t_1) & 0 & \cdots & 0 \\ a(t_2) & a(t_1) & \cdots & 0 \\ \vdots & \vdots & \ddots & \vdots \\ a(t_N) & a(t_{N-1}) & \cdots & a(t_1) \end{pmatrix}, \; \mathbf{c} = \begin{pmatrix} c(t_1) \\ \vdots \\ \vdots \\ c(t_N) \end{pmatrix}, \; \mathbf{r} = \begin{pmatrix} r(t_1) \\ \vdots \\ \vdots \\ r(t_N) \end{pmatrix}. \quad (1)$$

For example, CBF can be computed from $\mathbf{r}$ using the relationship $\mathrm{CBF} = \max \mathbf{r}(t) / \rho_{\mathrm{T}}$, where $\rho_{\mathrm{T}}$ denotes the tissue density. The residual function $\mathbf{r}$ can be recovered by solving the deconvolution problem

$$\mathbf{A}\mathbf{r} = \mathbf{c}. \quad (2)$$

However, the convolution matrix $\mathbf{A}$ is generally ill-conditioned [1]. Thus, slight errors in $\mathbf{c}$ (e.g., due to noise) result in large errors in $\mathbf{r}$ and solving LES 2 directly will result in physiologically not meaningful residual functions with strong oscillations and high energy. To obtain an improved solution, Tikhonov regularization can be applied, which penalizes solutions with a larger semi-norm $\|\mathbf{L}\mathbf{r}\|_2^2$

$$\mathbf{r}_\lambda = \arg\min_{\mathbf{r}} \; \|\mathbf{A}\mathbf{r} - \mathbf{c}\|_2^2 + \lambda^2 \|\mathbf{L}\mathbf{r}\|_2^2 . \quad (3)$$

The matrix $\mathbf{L} \in \mathbb{R}^{N \times N}$ typically describes a discrete approximation to some derivative operator. In standard Tikhonov regularization, as conducted in this work, $\mathbf{L}$ corresponds to the identity matrix $\mathbf{L} = \mathbf{I}$ (i.e., solutions with lower energy are preferred). The strength of regularization is controlled by the parameter $\lambda \in \mathbb{R}_{[0,\infty)}$. The quadratic optimization problem 3 can be solved using

singular value decomposition (SVD) [5], which decomposes $\mathbf{A}$ into the orthonormal left singular vectors $\mathbf{u}_i$, the orthonormal right singular vectors $\mathbf{v}_i$, and the non-negative singular values $\sigma_i$

$$\mathbf{A} = \sum_{i=1}^{N} \mathbf{u}_i \sigma_i \mathbf{v}_i^T \quad \text{with} \quad \sigma_1 \geq \sigma_2 \geq \ldots \geq \sigma_N \geq 0. \tag{4}$$

The regularized solution $\mathbf{r}_\lambda$ can be recovered using the SVD of $\mathbf{A}$ [5]

$$\mathbf{r}_\lambda = \sum_{i=1}^{N} f_i(\lambda) \frac{\mathbf{u}_i^T \mathbf{c}}{\sigma_i} \mathbf{v}_i \quad \text{with} \quad f_i = \frac{\sigma_i^2}{\sigma_i^2 + \lambda^2}. \tag{5}$$

### 2.2 Adaptive Regularization with the L-curve Criterion

The L-curve is a convenient way to display information about solutions computed via Tikhonov regularization [5]. It is a log-log plot of the norm of a regularized solution $\eta(\lambda)$ versus the norm of the corresponding residual norm $\rho(\lambda)$ (Fig. 1a). The quantities of $\eta(\lambda)$ and $\rho(\lambda)$ can be efficiently computed via the SVD of $\mathbf{A}$ [5]

$$\eta(\lambda) = \|\mathbf{r}_\lambda\|_2^2 = \sum_{i=1}^{N} \left( f_i(\lambda) \frac{\mathbf{u}_i^T \mathbf{c}}{\sigma_i} \right)^2 \tag{6}$$

$$\rho(\lambda) = \|\mathbf{A}\mathbf{r}_\lambda - \mathbf{c}\|_2^2 = \sum_{i=1}^{N} \left( (1 - f_i(\lambda)) \mathbf{u}_i^T \mathbf{c} \right)^2 \tag{7}$$

The L-curve criterion (LCC) states that the best trade-off between $\eta$ and $\rho$ is reached by a $\lambda$ lying on the characteristic corner of the L-curve. A corresponding

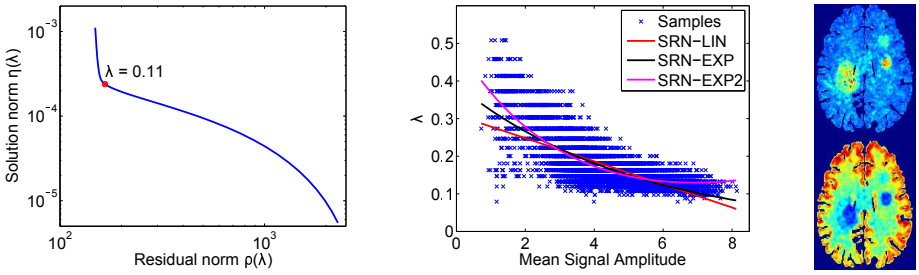


(a) (b) (c)

**Fig. 1.** (a) L-curve with $\lambda$ selected at maximum curvature; (b) mean signal amplitude $\bar{c}$ and corresponding $\lambda$ values determined using modified L-curve criterion (MLCC) (blue crosses) and corresponding regression functions using linear and exponential models; (c) top: plot of spatial distribution of $\lambda$ determined with MLCC, bottom: corresponding mean signal amplitude.

$\lambda$ can be found by identifying the maximum curvature $\kappa(\lambda)$ of the L-curve, where $\kappa(\lambda)$ is given as [5]

$$\kappa(\lambda) = 2\frac{\eta\rho}{\eta'}\frac{\lambda^2\eta'\rho + 2\lambda\eta\rho + \lambda^4\eta\eta'}{\left(\lambda^2\eta^2 + \rho^2\right)^{3/2}} \text{ with } \eta'(\lambda) = \sum_{i=1}^{N}(1-f_i)^2 f_i \mathbf{u}_i^T\mathbf{c}. \quad (8)$$

Salehi Ravesh et al. [4] discussed that the straightforward application of the LCC to MR lung perfusion data is not feasible. In many cases, $\kappa(\lambda)$ showed multiple maxima or no local maximum at all. In these cases, the $\lambda$ chosen by the LCC were too small leading to noisy results. Therefore a modified LCC (MLCC) was introduced implying two additional criteria: if multiple maxima are present in $\kappa(\lambda)$, the maximum with the largest $\lambda$ is chosen and if no local maximum is present, $\lambda$ is set to a minimally allowed value $\lambda_{\min} = 0.1 \cdot \sigma_1$.

### 2.3 Adaptive Regularization with SNR Regression

The LCC based methods require to sample $\kappa(\lambda)$ in a sufficient density. In practice, typically 50 evaluations of Equations 6, 7 and 8 are required to determine the parameter for computing the residual function for one tissue voxel. This causes a considerable amount of computational overhead. Figure 1c shows the average amplitude of the TCCs over time $\bar{c} = \frac{1}{N}\sum_{i=1}^{N} c(t_i)$, which is proportional to the average SNR, compared to the adaptive $\lambda$ values determined using the MLCC. As expected, higher $\lambda$ value were assigned to regions with low SNR and vice versa. This suggests to use simple regression functions to adapt the $\lambda$ values to the SNR. In this work, we apply a linear regression model (SNR-LIN), as well as exponential models with one (SNR-EXP) and two (SNR-EXP2) basis functions

$$\lambda_{\text{SNR-LIN}} = a\bar{c} + b, \qquad \lambda_{\text{SNR-EXP}} = a\exp(b\cdot\bar{c}), \qquad \lambda_{\text{SNR-EXP2}} = a\exp(b\cdot\bar{c}) + l\exp(m\cdot\bar{c}). \quad (9)$$

The regression parameters were computed using the `fit` function of the MATLAB curve fitting toolbox. Figure 1b shows examples for fitting the regression functions.

### 2.4 Evaluation Methods

For evaluation of the discussed methods, a volumetric time series of TCCs was simulated with a realistic numerical brain perfusion phantom [6]. The time series consisted of 3 slices with $256\times256$ voxels and 44 temporal samples with sampling distance $\Delta t = 1\,\text{s}$. Accordingly, white Gaussian noise with standard deviation $\sigma_\text{n} = 20\,\text{HU}$ was added and finally the TIPS method [7] was applied for noise reduction before perfusion parameter computation. The convolution matrix $\mathbf{A}$ was computed from the simulated ground truth AIF to avoid any influence from the AIF selection to the parameter computation. For quantitative evaluation,

**Table 1.** Estimated regression parameters according to the models in Equation 9 using different subsets of data.

| Method (Parameters) | Slice 1 | Slice 2 | Slice 3 | All slices |
|---|---|---|---|---|
| SNR-LIN $(a, b)$ | $(-0.30, 0.31)$ | $(-0.31, 0.31)$ | $(-0.31, 0.32)$ | $(-0.31, 0.31)$ |
| SNR-EXP $(a, b)$ | $(0.39, -0.19)$ | $(0.40, -0.20)$ | $(0.41, -0.20)$ | $(0.40, -0.20)$ |
| SNR-EXP2 $(a, b,$ $l, m)$ | $(0.50, -0.37,$ $0.04, 0.14)$ | $(0.50, -0.37,$ $0.03, 0.16)$ | $(0.51, -0.36,$ $0.03, 0.17)$ | $(0.50, -0.37,$ $0.03, 0.16)$ |

Lin's concordance correlation (CC) [8] between the computed values and the ground truth values in all tissue voxels was determined. In contrast to linear correlation the CC is sensitive to a shift and scaling in the estimates.

## 3 Results

Figure 2 shows CBF maps calculated with different methods and corresponding CC results. Table 1 shows the variation of the regression parameters using different subsets of the data.

## 4 Discussion

The CBF map in Figure 2 which was created using a high global regularization parameter $\lambda = 0.3$ results in a smooth map but severely underestimated CBF

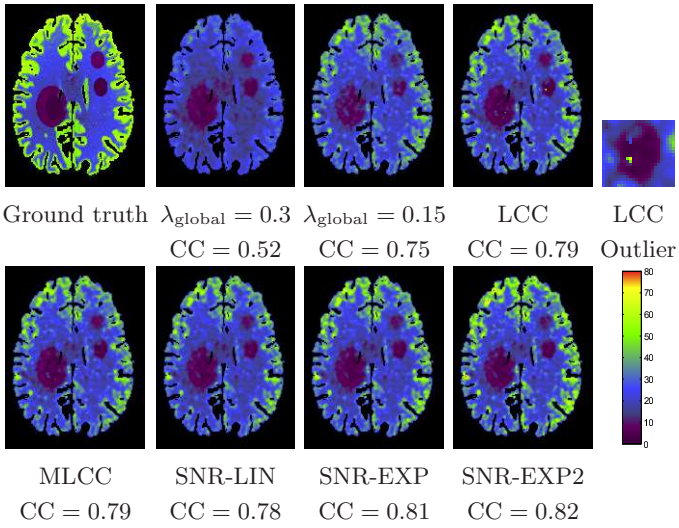


**Fig. 2.** CBF maps computed using Tikhonov regularization with global and adaptive parameter settings and the corresponding CC to the ground truth. Units: ml/100 g/min.

values. If a smaller $\lambda = 0.15$ is used, the CBF values are less underestimated but the map gets noisy and the areas with reduced perfusion values are not as well separated. The adaptive methods can achieve maps with limited noise and limited underestimation at the same time. LCC produces some few outliers, which can be avoided using the MLCC. The regression based methods show similarly improved results as the LCC methods, with the SNR-EXP2 method showing the overall best CC value. A limitation of this work is that the regression functions were fitted with the same data as they were applied to in the evaluation. However, Table 1 shows that the parameters only vary slightly for different subsets of the data. This suggests that the parameters are stable over different data sets, but needs to be evaluated closely in future research.

In summary, the results suggest that using simple regression functions to locally adapt the $\lambda$ parameter to the SNR can provide similar or even improved results compared to the computationally more expensive LCC based methods. From a clinical perspective, this approach could potentially provide quantitatively improved perfusion maps with less noise in a fast computation time.

Acknowledgments: The authors gratefully acknowledge funding of the Medical Valley, Erlangen, Germany, diagnostic imaging network, sub-project BD 16, grant nr. 13EX1212G.

## References

1. Fieselmann A, Kowarschik M, Ganguly A, Hornegger J, Fahrig R. Deconvolution-Based CT and MR Brain Perfusion Measurement: Theoretical Model Revisited and Practical Implementation Details; 2011. Article ID 467563, 20 pages. Int J Biomed Imaging.
2. Manhart M, Kowarschik M, Fieselmann A, Deuerling-Zheng Y, Royalty K, Maier AK, et al. Dynamic Iterative Reconstruction for Interventional 4-D C-Arm CT Perfusion Imaging. IEEE Trans Med Imaging. 2013 July;32(7):1336–1348.
3. Manhart M, Aichert A, Struffert T, Deuerling-Zheng Y, Kowarschik M, Maier AK, et al. Denoising and Artefact Reduction in Dynamic Flat Detector CT Perfusion Imaging using High Speed Acquisition: First Experimental and Clinical Results. Phys Med Biol. 2014 August;59(16):4505–4524.
4. Salehi Ravesh M, Brix G, Laun F, Kuder T, Puderbach M, Ley-Zaporozhan J, et al. Quantification of pulmonary microcirculation by dynamic contrast-enhanced magnetic resonance imaging: Comparison of four regularization methods. Magn Reson Med. 2013;69(1):188–199.
5. Hansen PC. The L-curve and its use in the numerical treatment of inverse problems. IMM, Department of Mathematical Modelling, Technical University of Denmark; 1999.
6. Riordan AJ, Prokop M, Viergever MA, Dankbaar JW, Smit EJ, de Jong HWAM. Validation of CT brain perfusion methods using a realistic dynamic head phantom. Med Phys. 2011;38(6):3212–3221.
7. Mendrik AM, Vonken E, van Ginneken B, de Jong HW, Riordan A, van Seeters T, et al. TIPS bilateral noise reduction in 4D CT perfusion scans produces high-quality cerebral blood flow maps. Phys Med Biol. 2011;56(13):3857–3872.
8. Lin LIK. A concordance correlation coefficient to evaluate reproducibility. Biometrics. 1989;45(1):255–268.